Journal of Alloys and Compounds 489 (2010) 469–474

Contents lists available at ScienceDirect

Journal of Alloys and Compounds

journal homepage: www.elsevier.com/locate/jallcom

Texture and orientation characteristics of α-Al_2O_3 films prepared by laser chemical vapor deposition using Nd:YAG laser

Akihiko Ito*, Hokuto Kadokura, Teiichi Kimura, Takashi Goto

Institute for Materials Research, Tohoku University, 2-1-1 Katahira, Aoba-ku, Sendai 980-8577, Japan

ARTICLE INFO

Article history:
Received 18 August 2009
Received in revised form
14 September 2009
Accepted 16 September 2009
Available online 23 September 2009

Keywords:
Laser CVD
Alumina
Coating
Orientation
Microstructure

ABSTRACT

α-Al_2O_3 films were prepared by laser chemical vapor deposition (LCVD) and the effects of precursor vaporization temperature (T_{vap}), total chamber pressure (P_{tot}), laser power (P_L) and deposition temperature (T_{dep}) on the phase, orientation and texture of Al_2O_3 film were investigated. At P_{tot} = 0.93 kPa, α-Al_2O_3 films were obtained in the region of T_{vap} > 423 K and T_{dep} > 1100 K. The orientation of α-Al_2O_3 film changed from (1 1 0) to (0 1 2) to (1 0 4) to (0 0 6) with increasing P_{tot}. Porous α-Al_2O_3 films were formed at high T_{vap} (443 K) and low P_{tot} (0.47 kPa). At T_{vap} = 413 K, α-Al_2O_3 film had hexagonal and rectangular plate-like grains with finely faceted edges. With increasing P_{tot} = 0.93–1.4 kPa, (0 0 6)-oriented α-Al_2O_3 film with a hexagonal terrace texture was obtained.

1. Introduction

Alumina (Al_2O_3) and titanium carbonitride (Ti(C, N)) are widely used as hard-coating materials. Since Al_2O_3 is characterized by high hardness and low thermal conductivity at high temperatures, the cutting efficiency and lifetime of cemented carbide (WC-Co) tools with an Al_2O_3 coating can be improved [1]. Moreover, since WC-Co tools should be able to withstand high temperatures and harsh stress conditions, when the dry cutting process with higher speed is employed, a high-performance hard coating is strongly demanded [2].

A low temperature deposition technique with phase control is required in Al_2O_3 coating due to the many polymorphs of Al_2O_3 [3]. In particular, among these polymorphs, corundum structure (α-phase) appears to be the only thermodynamically stable phase with excellent hardness at high temperatures. Although α-Al_2O_3 is widely used for hard-coating material [4], the deposition temperature of α-Al_2O_3 coating by conventional thermal chemical vapor deposition (CVD) is about 1273 K. Such high temperature restricts the selection of substrate to only a few materials with a high thermal stability. Metastable phases such as the γ- and κ-phases would have to be prepared at lower deposition temperatures. However, they may transform to the α-phase above 1000 K, resulting in volume change and cracking or delamination of the Al_2O_3 coating during the cutting process [5,6].

Several characteristics of α-Al_2O_3 coating such as hardness and roughness could depend on the crystallographic orientation and texture. Ruppi et al. prepared (0 1 2), (1 0 4), (0 0 1)-oriented α-Al_2O_3 films on Ti(C, O) and Ti(C, N) intermediate layers deposited on WC-Co substrate and reported that the films with (0 0 6) and (1 0 4) orientations showed higher hardness and modulus than those with random or the other orientations [4,7–9]. It is commonly understood that the crystal orientation depends not only on the substrate but also on the deposition temperature and the total pressure in the CVD process. Since α-Al_2O_3 film in a single phase can only be prepared at a high deposition temperature in a limited range by conventional thermal CVD, the relationship among deposition conditions, orientation and texture has not been studied in a wide range of conditions [1,10]. In order to develop an α-Al_2O_3 coating with control of phase, orientation and texture, a low temperature α-Al_2O_3 coating could be promising as a high-performance coating for cutting tools.

We have studied low temperature and high-speed deposition of thick Y_2O_3 and TiO_2 films with control of their orientations by laser CVD (LCVD) using a high-power Nd:YAG laser (260 W) [11,12]. In this study, we prepared α-Al_2O_3 films by LCVD and investigated the effect of deposition conditions on the phase, orientation and texture of Al_2O_3 film.

---

* Corresponding author. Tel.: +81 22 215 2106; fax: +81 22 215 2107.
E-mail address: itonium@imr.tohoku.ac.jp (A. Ito).

0925-8388/$ – see front matter © 2009 Elsevier B.V. All rights reserved.
doi:10.1016/j.jallcom.2009.09.088

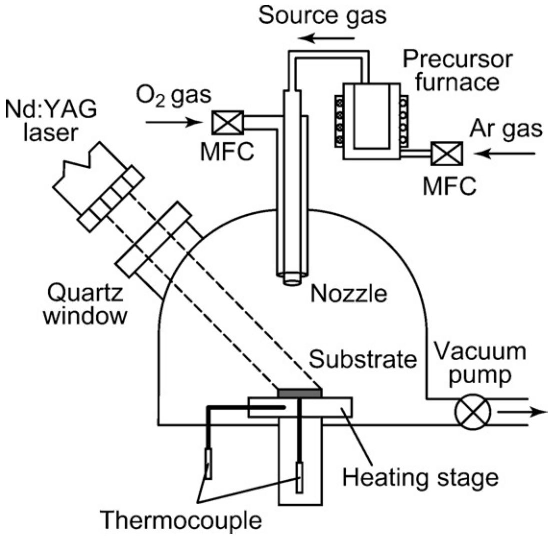

Fig. 1. Schematic of laser CVD apparatus.

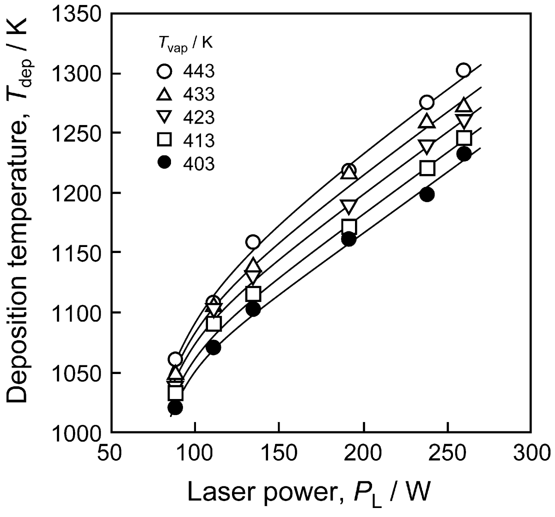

Fig. 2. P_L dependence on the T_{dep} at T_{pre} = 873 K, P_{tot} = 0.97 kPa and various T_{vap}.

2. Experimental procedure

Fig. 1 shows a schematic of the LCVD apparatus and Table 1 lists the deposition conditions. Aluminum tri-acetylacetonate ($Al(acac)_3$) was used as the precursor. $Al(acac)_3$ was vaporized at vaporization temperature (T_{vap}) of 453 K and carried into the CVD chamber with Ar gas. O_2 gas and $Al(acac)_3$ vapor were separately introduced into the CVD chamber through a double-tube nozzle. The gas flow rates of Ar and O_2 gases were maintained at 3.3×10^{-6} m^3 s^{-1} (200 sccm). The total pressure (P_{tot}) ranged from 0.47 to 2.33 kPa. Yttria-stabilized zirconia (YSZ) plates (12.5 mm × 12.5 mm × 1.0 mm) were used as the substrate, and the YSZ substrate was heated on a hot stage at pre-heating temperatures (T_{pre}) from room temperature to 973 K. The distance between the nozzle and the substrate was fixed at 28 mm. An Nd:YAG laser in a continuous wave mode (wavelength: 1064 nm) was collimated by lenses to irradiate the whole substrate and introduced into the CVD chamber through a quartz window. The laser power (P_L) was changed up to 260 W. The deposition temperature (T_{dep}) was measured with a thermocouple inserted into the back side of the substrate.

The crystal phase was determined by X-ray diffraction (θ–2θ XRD; Rigaku RAD-2C). The surface and cross-sectional texture was observed by scanning electron microscopy (SEM; Hitachi S-3100H). The deposition rate (R_{dep}) was calculated from the thickness and the deposition time.

3. Results and discussion

In common CVD process, T_{dep} is obviously one of the most dominant parameters and usually determined by heating with an electric current or by a high-frequency electromagnetic wave, etc. In the LCVD process, on the other hand, the T_{dep} can be determined for various parameters such as P_L, T_{pre}, P_{tot} and T_{vap}. For example, the P_L dependence on T_{dep} at various T_{vap} for T_{pre} = 873 K and P_{tot} = 0.97 kPa is depicted in Fig. 2. By laser irradiation, the T_{dep} increased by 150–200 K from T_{pre}, and the temperature increase from T_{pre} to T_{dep} became more than 400 K when the P_L was increased to 260 W. The temperature increase tended to be greater at higher T_{vap}. This might be caused by the increase in exothermic heat by the reaction between the precursor and O_2 gases as well as by the increase in significant plasma formation by laser irradiation of the gases.

Table 1
Deposition conditions.

$Al(acac)_3$ vaporization temperature (T_{vap})	403–443 K
Substrate pre-heating temperature (T_{pre})	873 K
Gas flow rate for both Ar and O_2 gases	3.3×10^{-6} m^3 s^{-1}
Total pressure (P_{tot})	0.47–2.33 kPa
Distance between nozzle and substrate	28 mm
Laser output power (P_L)	88–236 W

Fig. 3 shows the XRD patterns of Al_2O_3 films prepared at P_L = 192 W. At P_{tot} = 0.93 kPa and T_{vap} = 423 K (T_{dep} = 1210 K), α-Al_2O_3 film in a single phase with slight (0 1 2) and (1 0 4) orientation was obtained (Fig. 3(a)). At T_{vap} = 443 K, a peak around $2\theta = 41.7°$ (d = 0.217 nm) from the (0 0 6) plane was identified (Fig. 3(b)), its intensity increasing at P_{tot} = 1.4 kPa (Fig. 3(c)). The diffraction intensity of the (0 0 6) plane is only 2.0 compared with 100 for the (1 0 4) plane according to the JCPDS card (No. 46-1212). Therefore, the intensity of the (0 0 6) peak cannot be identified in common α-Al_2O_3. The Harris texture coefficient (TC) can be used to quantitatively estimate the orientation, particularly for a small diffraction

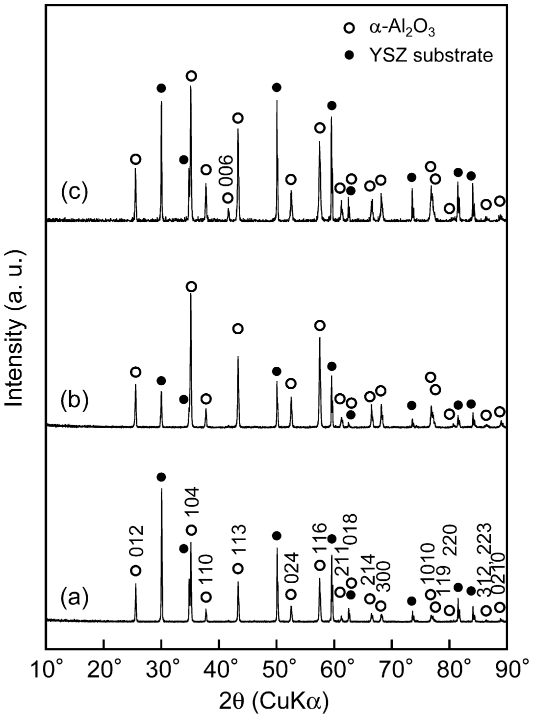

Fig. 3. XRD patterns of Al_2O_3 films prepared at P_L = 192 W, P_{tot} = 0.93 kPa and T_{vap} = 423 K (T_{dep} = 1210 K) (a), P_{tot} = 0.93 kPa and T_{vap} = 443 K (T_{dep} = 1230 K) (b), and P_{tot} = 1.4 kPa and T_{vap} = 443 K (T_{dep} = 1210 K) (c).

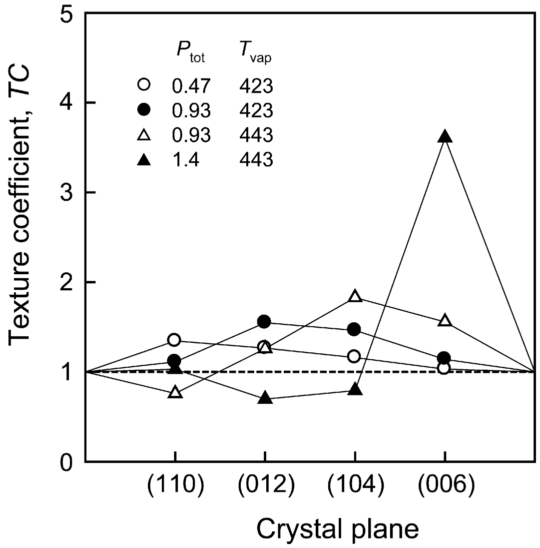

Fig. 4. Preferred orientations of Al_2O_3 films prepared at $P_L = 192$ W and various P_{tot} and T_{vap}: 0.47 kPa and 423 K (open circles), 0.93 kPa and 423 K (filled circles), 0.93 kPa and 443 K (open triangles), and 1.4 and 443 K (filled triangles).

peak [13].

$$\mathrm{TC}(h\,k\,l) = N\frac{I_\mathrm{m}(h\,k\,l)/I_0(h\,k\,l)}{\sum I_\mathrm{m}(h\,k\,l)/I_0(h\,k\,l)}, \qquad (1)$$

where $I_\mathrm{m}(h\,k\,l)$ and $I_0(h\,k\,l)$ are the intensity from the $(h\,k\,l)$ plane measured in the present study and that reported in JCPDS card (No. 46-1212), respectively. (0 1 2), (1 0 4), (1 1 0), (0 0 6), (1 1 3), (0 2 4), (1 1 6), (2 1 4) and (3 0 0) planes were used for the calculation ($N = 9$). TC$(h\,k\,l)$ has a value between 0 and N depending on the orientation degree of the $(h\,k\,l)$ plane. The TC of a non-oriented plane should be 1.0. If the TC is more than 1.0, we can define it as being oriented. If the TCs of more than two planes increase simultaneously, we can define them as being co-oriented. Fig. 4 shows the TC for (1 1 0), (0 1 2), (1 0 4) and (0 0 6) planes of α-Al_2O_3 films prepared at $P_L = 192$ W and various P_{tot} and T_{vap}. The α-Al_2O_3 film prepared at $P_{tot} = 0.47$ kPa and $T_{vap} = 423$ K was (1 1 0) and (0 1 2) co-oriented (open circles in Fig. 4), and that prepared at $P_{tot} = 0.93$ kPa was (0 1 2) and (1 0 4) co-oriented (filled circles in Fig. 4). At $P_{tot} = 0.93$ kPa and $T_{vap} = 443$ K, the α-Al_2O_3 film changed to (1 0 4) and (0 0 6) co-oriented (open triangles in Fig. 4). The α-Al_2O_3 film prepared at $T_{vap} = 443$ K and $P_{tot} = 1.4$ kPa was significantly (0 0 6) oriented (filled triangles in Fig. 4).

Fig. 5 depicts the effect of T_{dep} and T_{vap} on the phase formation of Al_2O_3 film. At $T_{dep} < 1060$ K, γ-Al_2O_3 films in a single phase were formed independently of T_{vap}. Al_2O_3 films with a $\gamma + \theta$ mixture phase were formed at $T_{vap} = 403$ K and $T_{dep} > 1070$ K, whereas Al_2O_3 films with an $\alpha + \theta$ mixture phase were formed at $T_{vap} = 413$ K and $T_{dep} > 1116$ K. At $T_{vap} > 423$ K, the phase changed from a γ to a $\gamma + \alpha$ mixture to an α-phase with increasing T_{dep}.

Fig. 6 depicts the effect of P_{tot} and T_{vap} on the phase and orientation of Al_2O_3 film. At $P_{tot} = 0.47$ kPa, α-Al_2O_3 film was prepared at $T_{vap} > 413$ K. With increasing T_{vap}, the orientation changed from (1 1 0) to (1 1 0) and (0 1 2) co-orientation to (1 0 4) and (0 1 2) co-orientation. At $P_{tot} = 0.93$ kPa, α-Al_2O_3 film was also prepared at $T_{vap} > 423$ K, and (0 1 2) and (1 0 4) co-oriented and (1 0 4) and (0 0 6) co-oriented α-Al_2O_3 films were prepared. A significant (0 0 6)-oriented α-Al_2O_3 film was obtained at $P_{tot} = 1.4$ kPa and $T_{vap} = 443$ K. At $P_{tot} > 1.9$ kPa and $T_{vap} < 423$ K, γ-Al_2O_3 film in a single phase was formed, and an α-phase appeared with a γ-phase at $T_{vap} > 433$ K. It can be summarized that at $T_{vap} > 423$ K, the Al_2O_3 film prepared at $P_{tot} < 0.93$ kPa tended to be α-phase, while the Al_2O_3 film at $P_{tot} > 1.4$ kPa tended to be γ-phase. At lower T_{vap}, a θ-phase appeared with the α- and γ-phases. The orientation of α-Al_2O_3 film changed from (1 1 0) to (0 1 2) to (1 0 4) to (0 0 6) with increasing P_{tot}.

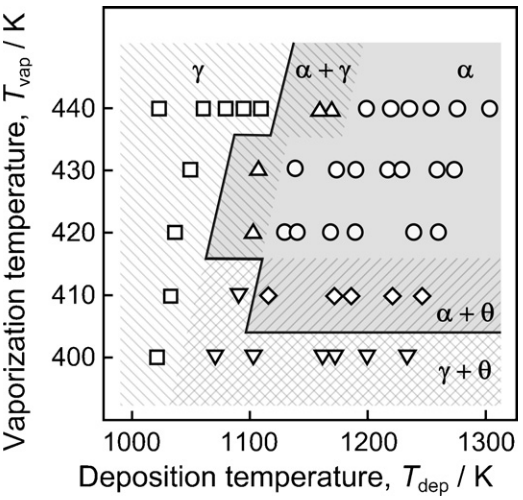

Fig. 5. Effect of T_{dep} and T_{vap} on the phase of Al_2O_3 films prepared at $P_{tot} = 0.93$ kPa.

Fig. 7 shows the surface SEM images of Al_2O_3 films prepared at various T_{vap}, P_{tot} and P_L. (1 0 4) and (0 0 6) co-oriented α-Al_2O_3 film prepared at $T_{vap} = 443$ K, $P_{tot} = 0.93$ kPa and $P_L = 192$ W had hexagonal faceted grains slightly inclined to the substrate (Fig. 7(a)). (0 0 6)-oriented Al_2O_3 film was obtained at $P_{tot} = 1.4$ kPa, and a hexagonal terrace texture developed on the surface of the grains (Fig. 7(b)). When the P_L increased to 238 W at $P_{tot} = 0.93$ kPa, rounded hexagonal and rectangular-shaped grains were observed (Fig. 7(c)). At $T_{vap} = 443$ K and $P_{tot} = 0.47$ kPa, porous α-Al_2O_3 film was formed (Fig. 7(d)). As in the conventional CVD process, a porous structure was often obtained under a high supersaturation condition of source gases. In the present study, the gas supply rate at $T_{vap} = 443$ K and $P_{tot} = 0.47$ kPa increased to a level two times higher than those of the other deposition conditions. When the T_{vap} decreased to 433 K, hexagonal and rectangular plate-like grains were grown with finely faceted edges (Fig. 7(e)). At $P_{tot} = 2.3$ kPa, γ-Al_2O_3 film having a cauliflower-like structure in a single phase was obtained (Fig. 7(f)). A typical cross-sectional SEM image of oriented α-Al_2O_3 films is shown in Fig. 8. The α-Al_2O_3 films with (1 0 4) and (0 0 6) co-orientation prepared at $T_{vap} = 433$ K, $P_{tot} = 0.93$ kPa and $P_L = 192$ W had a columnar structure. The step structure was

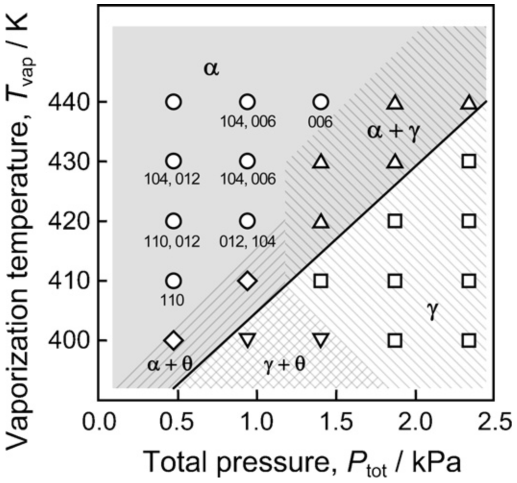

Fig. 6. Effect of P_{tot} and T_{vap} on the phase and orientation of Al_2O_3 films prepared at $P_L = 192$ W.

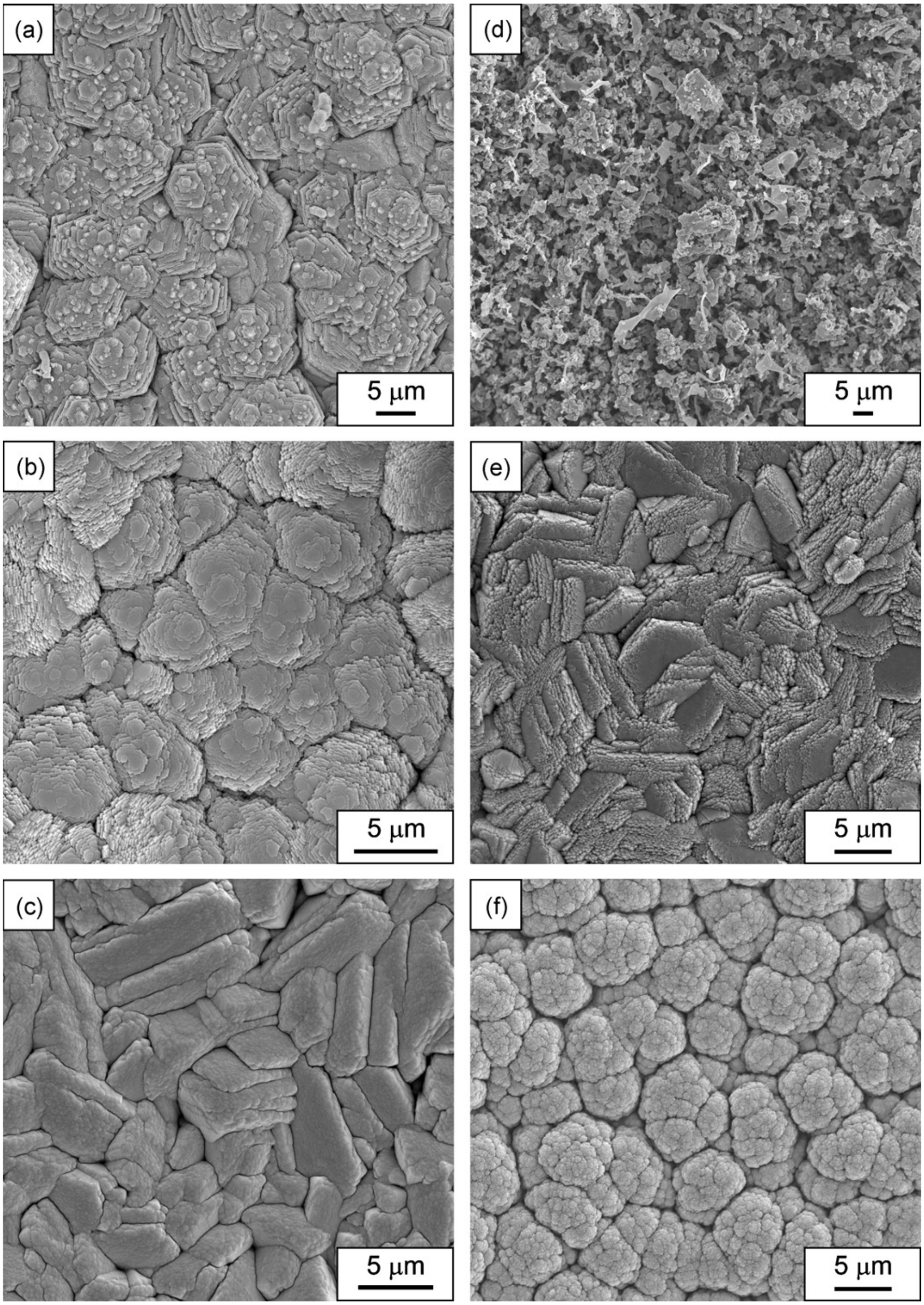

Fig. 7. Surface SEM images of Al_2O_3 films prepared at $T_{vap} = 443$ K and various P_{tot} and P_L: $P_{tot} = 0.93$ kPa and $P_L = 192$ W (a), $P_{tot} = 1.4$ kPa and $P_L = 192$ W (b), $P_{tot} = 0.93$ kPa K and $P_L = 238$ W (c), and at $P_L = 192$ W and various P_{tot} and T_{vap}: $P_{tot} = 0.47$ kPa and $T_{vap} = 443$ K (d), $P_{tot} = 0.47$ kPa and $T_{vap} = 433$ K (e), and $P_{tot} = 2.3$ kPa and $T_{vap} = 433$ K (f).

observed at the surface of columnar grains and the feather-like texture was formed in the cross-section. The thickness of the most α-Al_2O_3 films was ranging from 15 to 25 μm and the highest R_{dep} was 540 $\mu m\,h^{-1}$ at $T_{dep} = 1100$ K for γ-Al_2O_3 film, and was 324 $\mu m\,h^{-1}$ at $T_{dep} = 1200$ K for α-Al_2O_3 film.

Fig. 9 summarizes the effect of P_{tot} and T_{vap} on the texture of Al_2O_3 films prepared at various deposition conditions. At low P_{tot} (0.47 kPa) and high T_{vap} (443 K), porous α-Al_2O_3 film was formed. With increasing P_{tot} to 1.4 kPa, the α-Al_2O_3 film had columnar grains with a hexagonal terrace texture, while with decreasing T_{vap} to 413 K, α-Al_2O_3 film had hexagonal and rectangular plate-like grains with finely faceted edges. At higher P_{tot} or lower T_{vap}, γ- and θ-phases appeared with the α-phase, and non-oriented grains were grown with a hexagonal and rectangular faceted texture. At $P_{tot} > 1.4$ kPa, γ-Al_2O_3 film with a cauliflower-like texture was obtained.

The orientation and texture of α-Al_2O_3 film also depended on the deposition conditions such as T_{vap} and P_{tot}. Schematics of the cross-sectional crystal structure of the (0 0 6), (1 0 4), (0 1 2) and (1 1 0) planes of α-Al_2O_3 are presented in Fig. 10. In the corundum

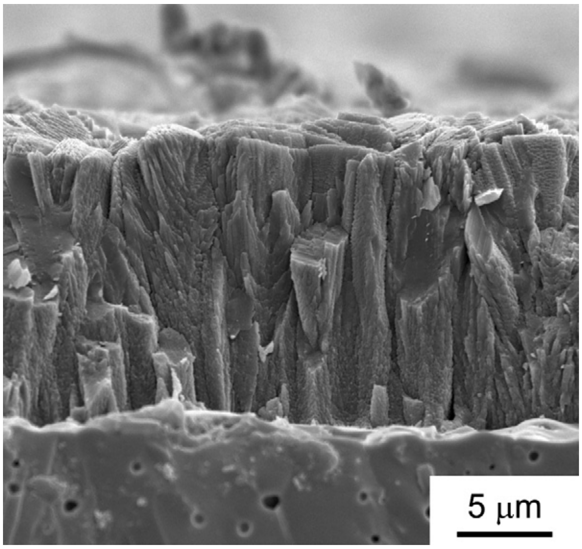

Fig. 8. Cross-sectional SEM image of α-Al_2O_3 films with (1 0 4) and (0 0 6) co-orientation prepared at T_{vap} = 433 K, P_{tot} = 0.93 kPa and P_L = 192 W.

structure of α-Al_2O_3, the Al_2O_9 octahedral dimers are joined alternately by edge- and corner-sharing in the *c*-axis direction. (0 1 2) and (1 0 4) planes intersect with the (0 0 6) plane at angles of 57.6° (Fig. 10(b)) and 38.2° (Fig. 10(c)), respectively. The orientation of α-Al_2O_3 film changed from (1 1 0) to (0 1 2) to (1 0 4) to (0 0 6) with increasing P_{tot}, as summarized in Fig. 5. It may be assumed that the longer direction of Al_2O_9 octahedral dimers (corresponding to the packing density of O^{2-} ions) decreased with increasing P_{tot} and T_{vap}. It is generally understood that the (0 0 1) orientation of hexagonal lattice would appear at a low supersaturation condition in vapor and liquid phase deposition in various systems. In the present LCVD, (0 0 6) oriented α-Al_2O_3 films were obtained under rather high P_{tot} conditions. Since homogeneous reactions in a gas phase (mainly powder formation) occurs more significantly at higher P_{tot}, resulting in depletion of source gases, supersaturation would be decreased with increasing P_{tot}. This might have caused the (0 0 6) orientation at high P_{tot}.

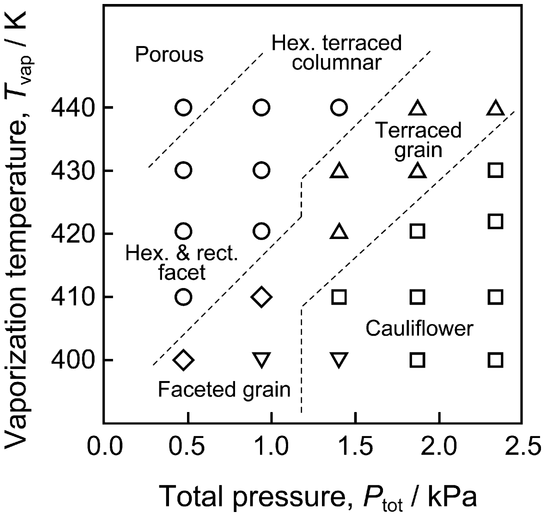

Fig. 9. Effect of P_{tot} and T_{vap} on the texture of Al_2O_3 films prepared at P_L = 192 W. Plot shapes correspond to the phase (Fig. 5).

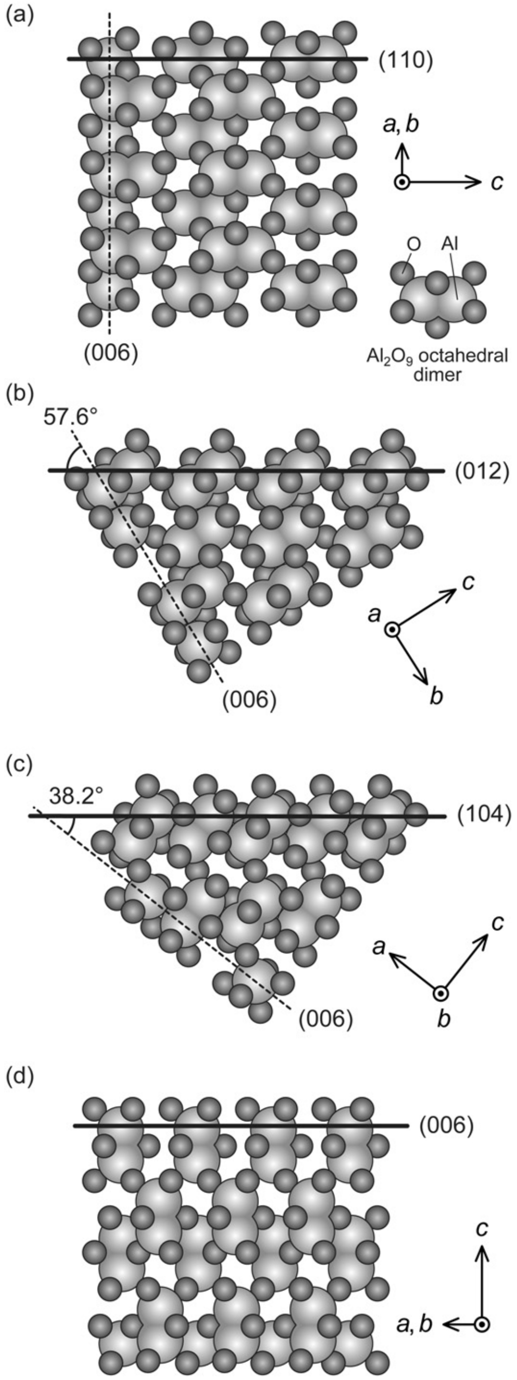

Fig. 10. Schematic of cross-sectional crystal structure of (0 0 6) (a), (1 0 4) (b), (0 1 2) (c) and (1 1 0) (d) planes of α-Al_2O_3.

4. Conclusions

α-Al_2O_3 films were prepared by LCVD and the effects of deposition conditions on the phase, orientation and texture of Al_2O_3 film were investigated. At P_{tot} = 0.93 kPa, α-Al_2O_3 films were obtained in the region of T_{vap} > 423 K and T_{dep} > 1100 K. The orientation of α-Al_2O_3 film changed from (1 1 0) to (0 1 2) to (1 0 4) to (0 0 6) with increasing P_{tot}. Porous α-Al_2O_3 film was formed at high T_{vap} (443 K) and low P_{tot} (0.47 kPa). When T_{vap} decreased to 413 K, α-Al_2O_3 film had hexagonal and rectangular plate-like grains with finely faceted edges, while with increasing P_{tot} = 0.93–1.4 kPa, (0 0 6)-oriented α-Al_2O_3 film with a hexagonal terrace texture was obtained.

Acknowledgements

This research was supported in part by the Global COE Program of Materials Integration, Tohoku University, and by the Asian CORE Program, Japan Society for the Promotion of Science (JSPS). This research was also performed as part of the Rare Metal Substitute Materials Development Project of the New Energy and Industrial Technology Development Organization (NEDO).

References

[1] B. Lux, C. Colombier, H. Altena, K. Stjernberg, Thin Solid Films 138 (1986) 49–64.
[2] H. Holleck, V. Schier, Surf. Coat. Technol. 76–77 (1995) 328–336.
[3] K. Wefers, C. Misra, Oxides and Hydroxides of Aluminium, Alcoa Laboratories, 1987.
[4] S. Ruppi, Surf. Coat. Technol. 202 (2008) 4257–4269.
[5] S. Vuorinen, L. Karlsson, Thin Solid Films 214 (1992) 132–143.
[6] M. Fallqvist, M. Olsson, S. Ruppi, Wear 263 (2007) 74–80.
[7] S. Ruppi, Int. J. Refract. Met. Hard Mater. 23 (2005) 306–316.
[8] S. Ruppi, A. Larsson, A. Flink, Thin Solid Films 516 (2008) 5959–5966.
[9] M. Fallqvist, M. Olsson, S. Ruppi, Surf. Coat. Technol. 202 (2007) 837–843.
[10] C.-S. Park, J.-G. Kim, J.S. Chun, J. Electrochem. Soc. 130 (1983) 1607–1611.
[11] T. Kimura, T. Goto, Mater. Trans. 44 (2003) 421–424.
[12] R. Banal, T. Kimura, T. Goto, Mater. Trans. 46 (2005) 2114–2116.
[13] C.S. Barrett, T.B. Massalski, Structure of Metals, 3rd ed., McGraw-Hill Book Company, Inc., New York, 1966.